applied sciences

MDPI

Article

Evolution of Residual Stress Based on Curvature Coupling in Multi-Roll Levelling

Guodong Yi *, Ye Liang, Chao Wang and Jinghua Xu *

State Key Laboratory of Fluid Power & Mechatronic Systems, Zhejiang University, Hangzhou 310027, China; liangye@zju.edu.cn (Y.L.); eg2013@zju.edu.cn (C.W.)

* Correspondence: ygd@zju.edu.cn (G.Y.); xujh@zju.edu.cn (J.X.); Tel.: +86-571-8795-1737 (G.Y. & J.X.)

Received: 2 September 2019; Accepted: 16 November 2019; Published: 19 November 2019

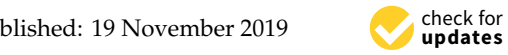

Abstract: Residual stress is the main cause of flatness defects in sheet metal and the basic method to improve the shape quality of the sheet is to reduce and eliminate the residual stress by multi-roll levelling. The curvature coupling between repeated sheet bendings in multi-roll levelling greatly affects the accuracy of the analysis of the residual stress evolution, which is rarely considered in current research. Aiming to address this problem, a method for eliminating residual stress by multi-roll levelling based on curvature coupling is discussed in this article. An evaluation criterion and an analysis model are proposed to investigate the evolution of the residual stress in multi-roll levelling considering the curvature coupling between bendings. The effects of the intermesh of the work rolls and the plastic deformation of the sheet on the residual stress are also discussed. The results show that multi-roll levelling will cause rolling residual stress while reducing the initial residual stress of the sheet and the larger plastic deformation caused by the intermesh of the work rolls at the entry is beneficial for the complete elimination of the initial residual stress, but the rolling residual stress will increase at the same time. Therefore, the total residual stress of the sheet after levelling depends on the appropriate levelling parameters.

Keywords: curvature coupling; residual stress; multi-roll levelling; sheet metal; work roll

1. Introduction

Rolling is a primary processing method for sheet metal, in which the inevitable internal stresses typically cause some explicit and implicit flatness defects [1]. An explicit defect means that the shape of the sheet is not an ideal plane because the longitudinal internal stress caused by the uneven distribution of the longitudinal fibre length of the sheet in the width direction exceeds the stress limit of the sheet. An implicit defect means that the sheet is flat in appearance, but when it is cut along the longitudinal direction, the explicit flatness defects reappear due to the release of internal stress [2–5]. The internal stress that causes the flatness defects of the sheet in rolling is called residual stress, which is a main factor affecting the quality of the sheet [6,7]. Therefore, reducing or eliminating residual stress as much as possible to improve the flatness of the sheet is the basis for ensuring that the quality of the sheet is good in subsequent processing [8].

The primary method of reducing and eliminating residual stress is multi-roll levelling. The basic principle of multi-roll levelling is that a series of alternating and progressively decreasing loads are applied to the sheet by a set of work rolls of the leveller to cause multiple elastoplastic deformations and the residual stress in the sheet is gradually reduced until it is eliminated [9,10].

The current research on analysis of the evolution of residual stress in multi-roll levelling mainly includes analytical methods, numerical methods, and experimental methods.

For analytical methods, Wang presented an iteration method with a relaxation factor to calculate the entry and exit stress variation of a cold rolling strip, considering the relationship between stress

variation and velocity variation and the incoming flatness propagation efficiency [11]. Kang et al. established a mechanical model of the strip to evaluate the distributions of contact pressure and residual stress of the strip, especially along the width direction, and calculated the longitudinal residual warpage accordingly by the virtual layers method [6]. Xue et al. presented a 3D axisymmetric elastic-plastic bending mathematical model of plates based on the Prandtle–Reuss increment theory according to the relevant initial conditions and boundary conditions of the plate and leveller to predict the residual stress and shape of the plate [12]. Liu et al. developed an analytical model with a computational procedure for describing the continuous bending, reversed bending process and the unloading process, evaluating the levelling process and residual stress distributions for typical H-beams [13]. Doege et al. developed an analytic forming model that analysed the roll levelling process with sufficient precision in a shorter time than is possible with the finite element method, investigating the states of multiple forming under bending conditions, and calculating the residual stresses and residual bend of the sheet metal [14].

For numerical methods, Abdelkhalek et al. calculated the shape and amplitude of the flatness defects of strips generated by residual stresses in strip rolling, with and without tension, by using a shell finite element model based on the asymptotic numerical method [7]. Weiss et al. analysed the rolling process using finite element analysis, determined the distribution of residual stresses, and obtained the theoretical moment curvature characteristics using the output of this analysis as the input to the modelling for pure bending [15]. Nakhoul et al. used a coupled finite element method to compute stresses and strains in-bite and out-of-bite in cold rolling of thin strips and predicted the manifested flatness defect, taking into account the stress field in the pre- and post-bite areas reorganized by the buckling [16]. Mathieu et al. introduced a numerical modelling of strip conveying through an industrial leveller using FEM software and predicted the final strip shape from plastic strains and residual stresses via width and thickness [17]. Abvabi et al. used numerical simulation to determine the influence of residual stress and the effect of plastic deformation on the material behaviour in roll forming, predicting the shape defects in the roll forming process if a residual stress profile exists in the material [18].

For experimental methods, the nanoindentation technique is widely used to examine the residual stresses distribution in the deformation machining process [19,20]. Sun et al. developed a slope cutting method for determining the residual stresses in roll formed products, which utilizes a modification of the current sectioning methods to obtain the membrane and bending residual stress components, and they employed a tapered removal approach to determine the layering stresses component by measuring the curvature variations of the remaining sample via its thickness direction [21].

The analytical methods predict the output variables by resolving the equations of the mathematical model that is almost instantaneous, however a complicated manufacturing process has to be simplified to a certain degree for mathematical modelling, which reduces the accuracy of the results. With the help of modern analysis software and hardware, finite element model may produce more accurate results but much slower in time. The experimental methods reveal the actual situation of the process, but lack of efficiency and have very high cost in capital and manpower. To take advantage of the benefits of each method, combinations of two or three of the methods may provide more information about the manufacture process.

In combinations of analytical methods and numerical methods, Quach et al. proposed an integrated analytical model and a closed-form solution for these residual stresses arising from the coiling and uncoiling process experienced by steel sheets before they become cold formed into sections and demonstrated the accuracy of the solution by comparing its predictions with those from a finite element simulation [22,23]. Silvestre et al. presented a semi-analytical model based on a discrete bending theory and classical beam theory for the process optimization of roll levelling, which is able to calculate the critical levelling parameters, i.e., force, plastification rate, and residual stresses, in a few seconds [24,25]. Nakhoul et al. studied a multi-scale method for modelling thin sheet buckling under residual stresses in the context of strip rolling and proposed a two-scale model based on the

generalized continuum approach for developing the unknowns in the Fourier series and solving von Karman equations of thin strip buckling in an energetic formulation [26]. Fischer et al. dealt with analytical and numerical considerations of buckling phenomena in thin plates under in-plane loads, which typically appear during the rolling and levelling of sheet metal, and investigated the buckling due to self-equilibrating residual stresses caused by the rolling process [2].

For combinations of analytical methods and experimental methods, Tan et al. expressed springback and residual stresses as a function of geometric parameters and material properties of sheet metals, determined the residual stresses using a layer-removing method, and carried out an analytical measurement of the residual stress by simulating the layer-removing process [27]. Zhang et al. developed a mathematical model to calculate the residual stress in stretched aluminium alloy thick plates based on the balance of stresses, two-dimensional plasticity, and a conception of free size, verifying the model against experiments performed on 7075 aluminium plates [28]. Milenin et al. developed a model of residual stresses in hot-rolled sheets based on the elastic-plastic material model, taking into account the nonuniform distribution of elastic-plastic deformations in the volume and unloading of the sheet material and phase transformation during cooling, and performed experimental verification of the model under industrial conditions [29]. Abvabi presented an inverse routine to predict residual stress in sheet material and collected data in a free bending test using the measurement of residual stress by X-ray diffraction to determine residual stress distribution in sheet material [30].

For combinations of numerical methods and experimental methods, Liu et al. carried out three-point cold bending experiments and tension tests on a thick steel plate, performing a numerical simulation with the finite element solver to replicate the experimentally determined residual stresses and strains [31]. Mehner and Milenin investigated the residual stress evolution of cold-rolled and hot-rolled steel sheets respectively by means of finite-element analysis simulations and X-ray diffraction [32,33]. LI et al. studied the numerical simulation of the tension levelling process of thin strip steel with the aid of finite element software, analysed the influence of the roll intermeshes in the anti-cambering on the distribution and magnitude of residual stresses in levelled strip steel, and carried out several experiments with the tension leveller based on the results from the simulation [34]. Tran et al. investigated the experimental and numerical modelling of flatness defects in strip cold rolling, proposed an experimental setup to analyse the interaction between residual stress and buckling for wavy edge flatness defects, and used finite element simulation for test validation [35,36]. Grüber et al. used a numerical model of a seven-roll leveller to determine roll positions resulting in a flat sheet and a defined residual stress distribution, measured the residual stresses across the sheet thickness after levelling using diffraction analysis [9,10].

In combinations of analytical methods, numerical methods, and experimental methods, the curvature integration method is a particularly noteworthy method. Liu et al. developed a mechanics model for predicting the levelling process of plates based on the curvature integration method and evaluated the residual stress using a global nonlinear unconstrained optimization method [8]. Cui et al. introduced the curvature integration by elastic-plastic differences to analyse the effect of bending on the levelling results and studied the plastic deformation ratio, residual stress, residual curvature, and levelling force for different levelling strategies to find an effectual strategy [37–39].

In multi-roll levelling, each elastoplastic bending deformation of the sheet will cause a change in the residual stress distribution, which in turn changes the curvature of the sheet and then affects the distribution of residual stress again. Therefore, the evolution of the residual stress of the sheet in multi-roll levelling is a multi-factor coupled process, which is particularly closely related to the bending curvature. However, there are few studies on the curvature coupling between bendings. In addition, improper parameter settings in multi-roll levelling of the sheet not only do not reduce the residual stress but also cause new residual stress. The previous research is mainly focused on eliminating the initial residual stress of the sheet and the new residual stress caused by the plastic deformation during the levelling process has not received enough attention. Some studies analyse the initial residual stress

evaluation of the sheet in multi-roll levelling, but the systematic calculation method of the residual stress after levelling is not proposed, and the key factors affecting the residual stress are not discussed.

Based on the coupled curvature integral model, this article analyses the evolution of the residual stress in multi-roll levelling, proposes the evaluation criteria and calculation model of the residual stress, discusses the key levelling parameters affecting the residual stress, and provides support for the design of the multi-roll levellers as well as the adjustment of the process parameters.

2. Residual Stress in Multi-Roll Levelling

During the multi-roll straightening process, the sheet metal is bent by the upper and lower work rolls, resulting in multiple alternating elastoplastic bending deformations, as shown in Figure 1. Considering the bending radius is much larger than the thickness of the sheet, the modelling of the levelling process is based on simple bending theory [14], thus, some basic assumptions are applied: (1) The cross sections remain on a plane and only rotate along the intersection lines with neutral layer during bending; (2) the strain neutral layer and stress neutral layer always coincide with the geometric centre layer of the sheet section during deformation; and (3) the stress state of any mass point on the cross section is uniaxial stretching or compression.

Based on the above assumptions, the bending process gives rise to a symmetric strain distribution along the sheet thickness [25]. If the bending radius is ρ and the curvature is A, the strain of the fibre with a distance z from the neural layer can be expressed as,

$$\varepsilon_z = (\rho + z)A - \rho A = zA \tag{1}$$

If the strain of the surface fibre reaches elastic limit ε_e, the current curvature A_t is called the elastic limit curvature:

$$A_t = \frac{2\varepsilon_e}{H} \tag{2}$$

The elastic limit stress σ_e and yield limit stress σ_s of typical elastoplastic materials are very close, thus $\varepsilon_e = \sigma_e/E = \sigma_s/E$, E is the Young's elastic modulus. When the bending curvature exceeds A_t, the outer material will be plastically deformed. H_t denotes the distance from the elastic-plastic demarcation point to the neutral layer at which the strain reaches ε_e. Then, the elastic region is between 0 and H_t, and the plastic region is between H_t and $H/2$. The elastoplastic deformations occur only in the area before the sheet metal contacts the roller. A_i represents the curvature of each bending at the contact point between the metal sheet and roller.

Applying a certain degree of plastic deformation is considered an effective method to reduce residual stress [40]. The mechanism of this phenomenon is that the grain sliding during the plastic deformation can alleviate the misfits between different regions or between different phases within the material, resulting in stress relaxation [41,42]. Experimental studies have also shown that when the material strain reaches the yield limit, the residual stress is significantly reduced [43,44]. Based on these results, in our model, the residual stress in the plastic deformation region before each bending is considered to be eliminated by the following bending. Correspondingly, the residual stress in the elastic region remains unchanged.

For each bending, the next bending is a reverse one, therefore, from the contact point with roller i to the contact point with roller $i+1$ the sheet curvature will have a continuous change from A_i to zero and from zero to A_{i+1}, during which both the plastic and elastic regions will have a springback process. If the material at the different layers springback freely, the material in elastic region returns to the initial position, and the material in plastic region returns to the position by a certain springback ε_e. However, the deformation of the material must meet the deformation coordination condition to keep the cross sections on a plane, which means the two regions interact with each other in the springback. The permanent plastic deformation will hold the elastic region, prevent it from full springback, and the rebounding stress of elastic region will also force the plastic region to cause excessive springback [45]. Such interaction leads to new internal stresses, that is, rolling residual stress. The final residual stress

after levelling is the superposition of initial residual stress and the rolling residual stress. Although the distribution of initial residual stress is uneven and irregular along the thickness of the sheet metal, it will be substantially eliminated in the first bending and most of the residual stress after levelling is due to the rolling process. The rolling residual stress symmetrically distributed along the thickness can be modelled and evaluated by analysing the deformation rule of the multi-roll levelling process [8,14].

As mentioned above, the key factor that affects the elastoplastic deformation is the curvature A_i. Based on previous experiments and simulation studies, during the alternative bending process in which the curvature A_i is gradually reduced, the residual stress is also gradually reduced and homogenised [8,46].

The calculation of A_i is based on the coupled curvature integral model. This model is composed by a geometric model and a bending moment curvature model, where the former describes the relationship between the intermesh and the curvature, while the latter expresses the relationship between the bending moment and the curvature. The modification of this model is to consider the influence of the residual curvature of the previous bending on the subsequent bending, which improves the accuracy of the model. The construction and solution of the model is not the focus of this study and will be described separately.

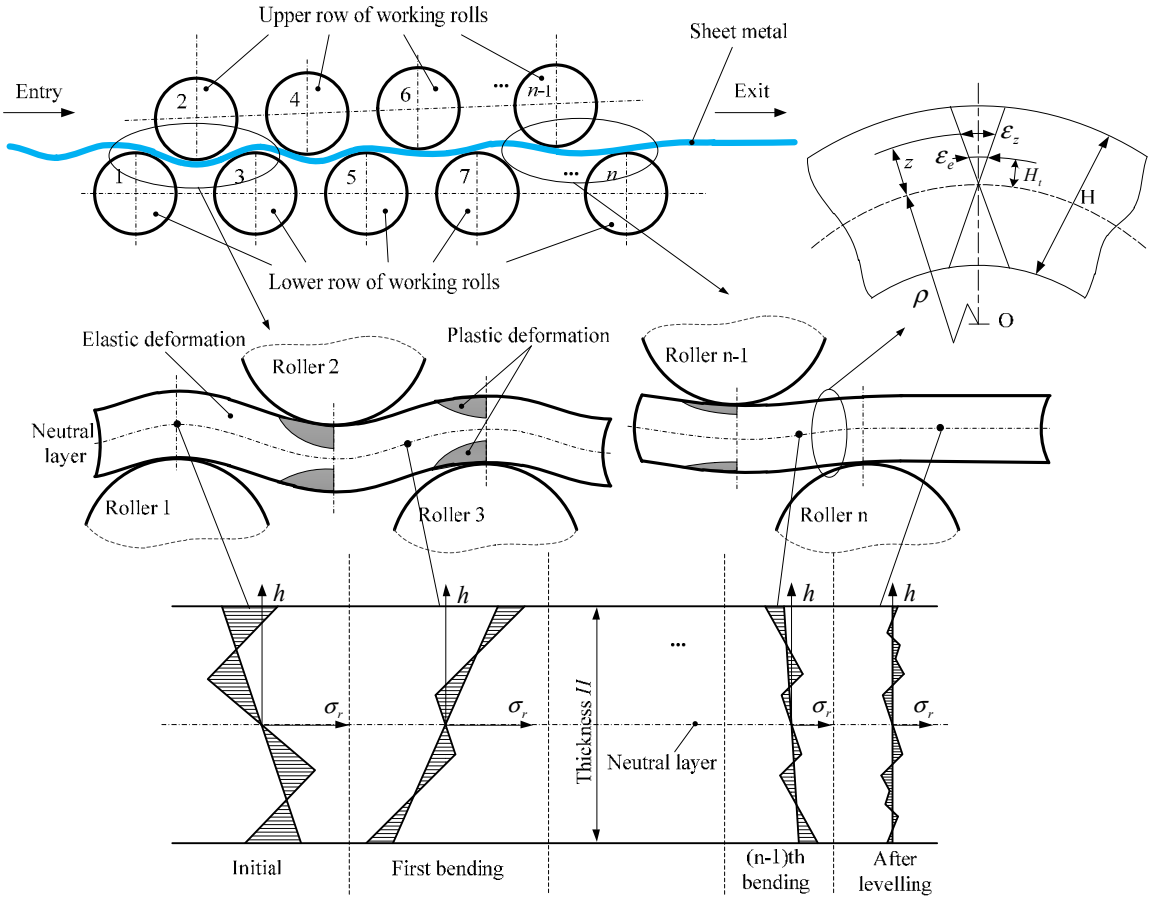

Figure 1. Variation of the residual stress in multi-roll levelling.

3. Evaluation Criteria for Residual Stress

To examine the residual stress comprehensively from a macroscopic perspective, it is necessary to establish an evaluation criterion for residual stress. The distribution of residual stress along the thickness is shown in Figure 2. The initial residual stress before levelling is uncertain because it depends on the initial condition of the sheet. However it has no influence on the generation of rolling residual stress and will be substantially eliminated in the first bending whether it is compressive or

tensile. Thus, the uncertainty of the initial residual stress has little effect on the evaluation of residual stress. The distribution of the residual stress after levelling typically consists of line segments and each of them corresponds to a reverse bending of the sheet performed by a work roll. Each part of the residual stress can be compressive or tensile, but we only consider the magnitude of the value. In this article, the absolute mean value $\overline{|\sigma_r|}$ of the residual stress is used as the evaluation criterion to describe the overall characteristics of the residual stress of the sheet. In Figure 2, the coordinates of a point T on the lines of the residual stress are $(\sigma_r(h), h)$ and $\overline{|\sigma_r|}$ is calculated by the following integral:

$$\overline{|\sigma_r|} = \frac{1}{H}\int_{-H/2}^{H/2} \left|\sigma_r(h)\right| dh \tag{3}$$

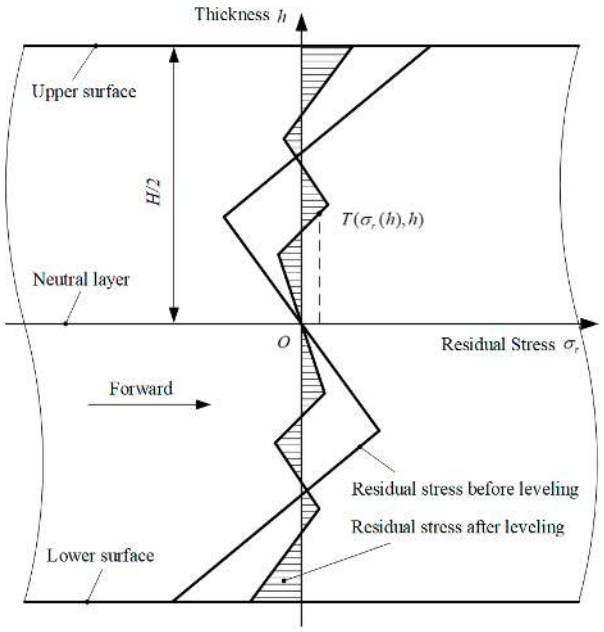

Figure 2. Distribution of the residual stresses before and after levelling.

4. Evolution of the Residual Stress in Multi-Roll Levelling

The sheet is typically bent many times in multi-roll levelling. Most of the bendings cause elastoplastic deformation, which further causes the redistribution of residual stress. Therefore, the distribution of residual stress is dynamically evolved.

Since no tension acts on the sheet in multi-roll levelling, the neutral layer of the sheet remains at the centre of the thickness in the elastoplastic deformation of the repeated bending. In addition, the distribution of the initial residual stress in the sheet is very close to the anti-symmetry in the thickness direction after elastoplastic bending, so a half-thickness sheet is taken as the analysis object.

The evolution of residual stress includes two main stages, i.e., the stage of the first bending and the stage from the second to the last bending, and the residual stress evolution of each bending in the latter is similar.

4.1. Evolution of the Residual Stress in the First Bending

There are two cases of the residual stress evolution in the first bending depending on whether the sheet contains initial residual stress. The case of no initial residual stress is shown in Figure 3a, where a half-thickness sheet is used as an analysis object, the abscissa indicates strain, and the ordinate indicates thickness. OA_c^0 represents the strain distribution corresponding to the initial residual curvature of the sheet and OA_{N+1} represents the strain distribution corresponding to the curvature of the first valid bending. The first valid bending refers to the bending that causes the maximum strain of the sheet

with the initial curvature. Only the first and subsequent bendings are significant for the evolution of the residual stress because the effect of the previous bending on the sheet will be eliminated as an initial residual stress. The first bending in this article refers to the first valid bending and N is the number of instances of bending before the first valid bending.

H_t^1 is defined as the thickness of the elastic region of the sheet corresponding to the first bending then, the elastic region is between 0 and H_t^1, and the plastic region is between H_t^1 and $H/2$. If the sheet is bent to the position OA_{N+1} and then the external force is removed, a free springback will be presented. If the interaction between the two regions in the springback is not taken into account, the elastic region OB returns to the initial position OO_1 by a full springback, and the plastic region BA_{N+1} returns to the position $O_1A_c^{(N+1)'}$ by a certain springback. ε_e. ε_e is the elastic strain limit, that is, the strain when the sheet is bent from the free state to the critical position of the elastic region and the plastic region. The lines that indicate the free position of the sheet under stress-free conditions similar to $OO_1A_c^{(N+1)'}$ are defined herein as the initial line. However, because the two regions interact with each other in the springback, the actual springback position of the sheet that satisfies the deformation coordination condition is located at line OA_c^{N+1} instead of $OO_1A_c^{(N+1)'}$. The inconsistency between the unstressed free position $OO_1A_c^{(N+1)'}$ and the actual position OA_c^{N+1} forms an internal stress region, including a compressive stress region OO_1P_1 and a tensile stress region $P_1A_c^{N+1}A_c^{(N+1)'}$. The numbers above the lines OA_c^0, OA_{N+1}, and OA_c^{N+1} indicate the order of bending and springback of the sheet.

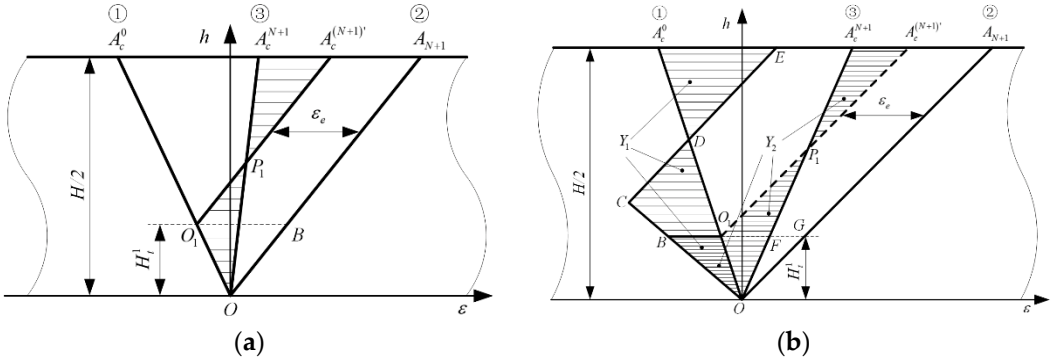

Figure 3. Evolution of residual stress in the first bending. (**a**) A sheet without initial residual stress and (**b**) a sheet with initial residual stress.

According to the above-mentioned analysis, a sheet without initial residual stress exhibits internal stress caused after the first bending. Therefore, the internal stress of the sheet due to the roll levelling is defined as the rolling residual stress to distinguish it from the initial residual stress.

The springback of the sheet with initial residual stress is similar to that without residual stress, as shown in Figure 3b. Y_1 represents the initial residual stress of the sheet, including two regions, OCD and DEA_c^0, which are tensile stress and compressive stress, respectively. If the sheet is bent from the initial position OA_c^0 to position OA_{N+1} and then the external force is removed, the elastic region OG returns to the initial position OO_1 with a free springback, the plastic section GA_{N+1} returns to the position $O_1A_c^{(N+1)'}$ with a springback ε_e, and finally the sheet returns to the position OA_c^{N+1} due to the deformation coordination, accompanied by a certain residual stress. Y_2 represents the residual stress after the first bending, including three triangular regions, where OO_1P_1 and $P_1A_c^{N+1}A_c^{(N+1)'}$ are residual stresses caused by roll levelling and OO_1B is the internal stress left by the initial residual stress. During the bending process, OO_1B is always in the elastic region and remains unchanged in the initial state due to no plastic deformation, while O_1BCD and DEA_c^0 in the plastic region all disappear and are replaced by the residual stress caused by roll levelling.

According to the two cases of the first bending described above, the following results are obtained. In the plastic region, there are only rolling residual stresses in both cases and the stress distributions

are the same. In the elastic region, the distributions of the rolling residual stress are the same in both cases, but if there is an initial residual stress, the part in the elastic region of it cannot be eliminated (the residual stress corresponding to the region OO_1B in Figure 3b), which is also the only trace of initial residual stress left after levelling.

Therefore, the characteristics of the first bending in multi-roll levelling are as follows. First, the roll levelling will cause some residual stresses. Second, the initial residual stress in the elastic region remains unchanged, while the initial residual stress in the plastic region is completely eliminated. Thus, if the plastic deformation region of the first bending is large enough, most of the initial residual stress will be eliminated. However, large plastic deformation causes large rolling residual stress and eventually the total residual stress cannot be effectively reduced.

4.2. Evolution of Residual Stress in Multiple Bendings

The evolution of residual stress in each bending after the first bending is similar and the second bending is analysed first. Figure 4 demonstrates the evolution process of residual stress for the second bending on the basis of the first bending, shown in Figure 3b, with the same initial residual stress. The second bending starts from the springback position OA_c^{N+1} after the first bending to the position OA_{N+2} and ends with a springback, which also includes the elastic region and plastic region. The elastic region is between 0 and H_t^2, and the plastic region is between H_t^2 and $H/2$. Due to the gradual decrease of the intermeshing of the of the work rolls in multi-roll levelling, the bending curvature is gradually decreased, and the elastic region is gradually increased, that is, $H_t^1 < H_t^2$.

In the second springback, the elastic region OB returns to the initial position OO_1O_2 after the first springback and the plastic region BA_{N+2} returns to $O_2A_c^{(N+2)'}$ by a springback ε_e. Thus, after the second springback, the initial line for free position is $OO_1O_2A_c^{(N+2)'}$, and the final springback position is OA_c^{N+2} due to the deformation coordination also. The residual stress at this time is three triangular regions surrounded by $OO_1O_2A_c^{(N+2)'}$ and OA_c^{N+2}, wherein the triangles OO_1P_1 and $P_2A_c^{(N+2)'}A_c^{N+2}$ represent tensile stress and P_1P_2O represents compressive stress.

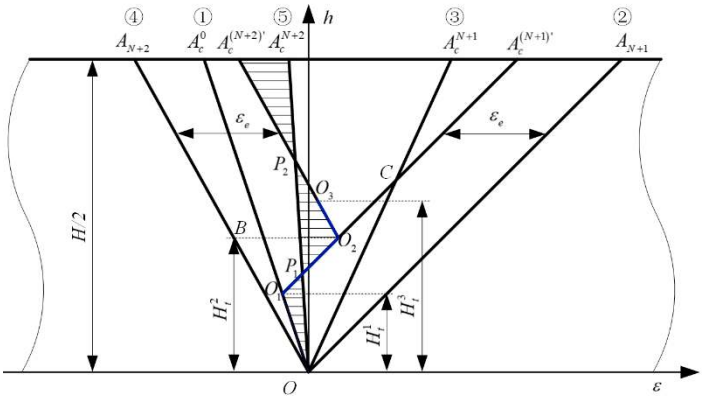

Figure 4. Evolution of residual stress in the second bending.

In Figure 4, the rolling residual stress after the first bending corresponds to the triangles OO_1C and $CA_c^{N+1}A_c^{(N+1)'}$, and the rolling residual stress after the second reverse bending corresponds to the triangles OO_1P_1, P_1P_2O, and $P_2A_c^{(N+2)'}A_c^{N+2}$. Since the absolute mean value $\overline{|\sigma_r|}$ of the residual stress is proportional to the area of the shadow in the figure, the rolling residual stress after the second bending is found to be smaller than after the first bending by comparing the areas of the triangles. The main concern of the second bending process is the rolling residual stress caused by multi-roll levelling. As for the initial residual stress, the portion distributed in the plastic region has been eliminated in the first bending, and the portion distributed in the elastic region cannot be changed in the second and subsequent bendings. Therefore, the first bending is the only chance to eliminate the

initial residual stress and the subsequent bendings can only reduce the rolling residual stress caused by the first bending.

The third bending is similar to the second one. The thickness of the elastic region increases again, from H_t^2 to H_t^3. At this time, the initial line is $OO_1O_2O_3A_c^{(N+3)'}$, and the corresponding distribution of residual stress becomes a region surrounded by $OO_1O_2O_3A_c^{(N+3)'}$ and OA_c^{N+3}. For the i-th bending, the distribution of residual stress is the region surrounded by $OO_1 \cdots O_iA_c^{(N+i)'}$ and OA_c^{N+i}.

Figure 5 demonstrates the evolution of residual stress in the multi-roll levelling of a sheet. After the first bending, the initial residual stress in the elastic region is maintained, the initial residual stress in the plastic region is eliminated, and a new rolling residual stress is caused. The second and subsequent bendings gradually reduce the rolling residual stress but have no effect on the remaining initial residual stress in the elastic region.

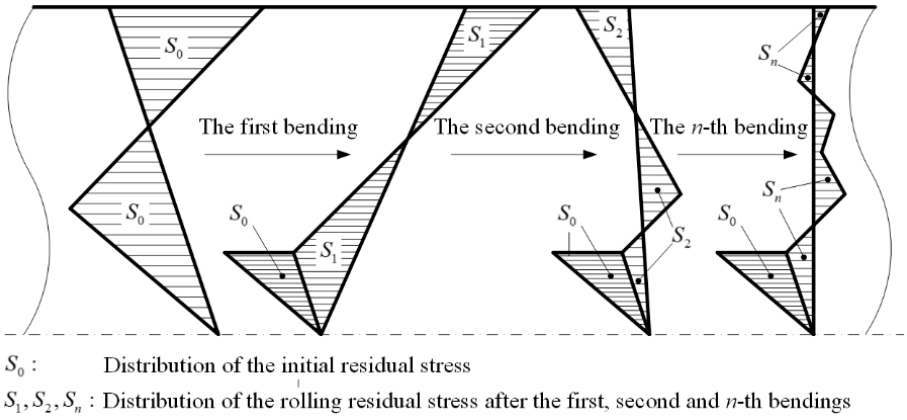

Figure 5. Evolution process of the residual stress in multi-roll levelling.

5. Modelling and Calculation of Residual Stress

The total residual stress of the sheet after levelling consists of two parts: One is the rolling residual stress caused by multi-roll levelling, which is distributed over the entire thickness direction of the sheet and the other is the remaining part of the initial residual stress, which is only distributed in the elastic region of the first valid bending.

The calculation model of the rolling residual stress is shown in Figure 6. According to the evolution rule of the residual stress of the sheet in multi-roll levelling, the distribution of the final rolling residual stress after the m-th valid bending is the region surrounded by $OO_1 \cdots O_mA_c^{(N+m)'}$ and OA_c^{N+m}. For the convenience of calculation, the abscissa and the ordinate are divided by ε_e and $H/2$, respectively, with the coordinate interchanging. The residual stress distribution after coordinate interchange is shown in Figure 6, where $OO_1 \cdots O_mO_{m+1}$ (which should be $OO_1 \cdots O_mA_c^{(N+m)'}$ according to the naming rules in Figure 4, and O_{m+1} is an alias of $A_c^{(N+m)'}$ for modelling uniformity) represents the initial position and OP_{m+1} (which should be OA_c^{N+m} and P_{m+1} is an alias of A_c^{N+m}) represents the actual stress distribution after the last bending and springback. The sheet after levelling is nearly flat, so the strain at point P_{m+1} is close to zero. If the sheet is completely flat, P_{m+1} is on the abscissa axis. Since the plate thickness has been normalised, the absolute mean value $\overline{|\sigma_r|}$ of the residual stress is the product of the shaded area in Figure 6 and the stress yield limit σ_s, that is:

$$\overline{|\sigma_r|} = \frac{1}{H}\int_{-H/2}^{H/2}\left|\sigma_r(h)\right|dh = \sigma_s\sum_{i=0}^{m+1} f_i \tag{4}$$

where f_i is the area of the region with residual stress distribution between the i-th turning point O_i and the i+1-th turning point O_{i+1}, which is determined by the line OP_{m+1}, and the turning points O_i.

The residual curvature after levelling is calculated by the bending moment curvature model, so OP_{m+1} is determined, but the coordinates of O_i need to be further calculated.

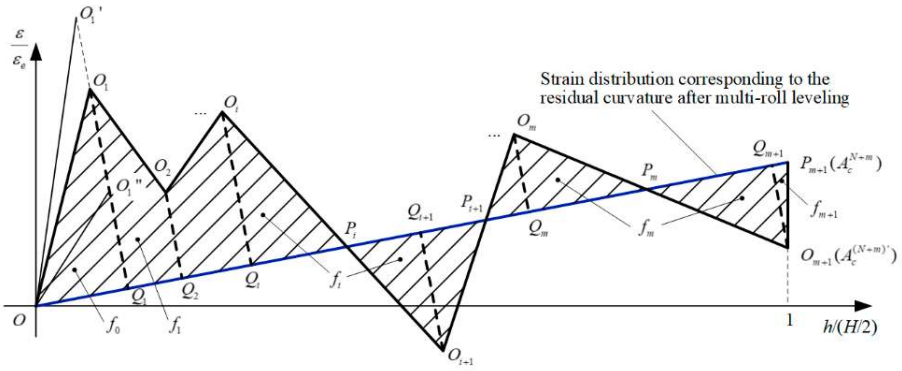

Figure 6. Distribution of the residual stress after multi-roll levelling.

According to Figure 4, the line equation of the strain line corresponding to the curvature of the i-th valid bending in Figure 6 is:

$$y = k_{N+i}x \tag{5}$$

where,

$$k_{N+i} = \frac{A_{N+1}}{A_t} \tag{6}$$

The line $O_iA_c^{(N+i)'}$ (i.e., O_iO_{i+1}) is obtained by translating the line OA_{N+i} in the y direction with distance 1, and the equation is:

$$y = k_{N+i}x + (-1)^{N+i+1} \tag{7}$$

When $i \geq 2$, O_i is the intersection of line $O_iA_c^{(N+i)'}$ and line $O_{i+1}A_c^{(N+i+1)'}$, and Equation (8) is obtained according to Equation (7):

$$\begin{cases} y = k_{N+i}x + (-1)^{N+i+1} \\ y = k_{N+i+1}x + (-1)^{N+i} \end{cases} \tag{8}$$

The solution to Equation (8) is the coordinate (x_i, y_i) of O_i, which is solved as follows:

$$\begin{cases} x_i = (-1)^{N+i+1}\frac{2}{k_{N+i+1}-k_{N+i}} \\ y_i = (-1)^{N+i+1}\frac{k_{N+i+1}+k_{N+i}}{k_{N+i+1}-k_{N+i}} \end{cases} \tag{9}$$

When $i = 1$, O_1 is on the line OA_c^0 and at the abscissa position of O_1, the difference between line OA_c^0 and line OA_{N+1} is exactly 1. Then,

$$\begin{cases} y_1 = k_0x_1 \\ y_1 + (-1)^{N+1} = k_1x_1 \end{cases} \tag{10}$$

The equation for line OP_{m+1} is $y = k_nx$ and Q_i is the foot of O_i to line OP_{m+1}. The coordinate $\left(x_i^q, y_i^q\right)$ of point Q_i is:

$$\begin{cases} x_i^q = \frac{k_ny_i+x_i}{k_n^2+1} \\ y_i^q = \frac{k_n^2y_i+k_nx_i}{k_n^2+1} \end{cases} \tag{11}$$

When point O_i and point O_{i+1} are on opposite sides of line OP_{m+1}, P_i is the intersection of line O_iO_{i+1} and line OP_{m+1}, and its coordinate $\left(x_i^p, y_i^p\right)$ is:

$$\begin{cases} x_i^p = (-1)^{N+i+1} \frac{1}{k_n - k_{N+i}} \\ y_i^p = (-1)^{N+i+1} \frac{k_n}{k_n - k_{N+i}} \end{cases} \tag{12}$$

Equation (9) to (12) determine the calculation methods for points O through O_{m+1}, Q_1 through Q_{m+1}, and P_1 through P_{m+1}. All of the slopes $k_0, k_1, \ldots, k_n$ are solved by calculating the ratio of the curvature at the contact point of each roll to the elastic curvature limit via the coupled curvature integral model. After the coordinates of these points are determined, the area f_i of each part can be solved. When O_i and O_{i+1} are on the same side and opposite sides of the line OP_{m+1}, f_i is a trapezoidal region and two triangular regions, respectively. The method for determining the position of point O_i and point O_{i+1} is that the coordinates of the two points are substituted into the equation of line OP_{m+1} and their product is calculated by Equation (13):

$$g = (y_{i+1} - k_n x_{i+1})(y_i - k_n x_i) \tag{13}$$

They are on the same side if $g > 0$ and on opposite sides if $g < 0$. According to Figure 6, f_i is calculated by Equation (14):

$$\begin{cases} f_0 = \frac{1}{2}|OQ_1| \cdot |O_1Q_1| \\ \begin{cases} f_i = \frac{1}{2}\left(|O_iQ_i| + \left|O_{i+1}Q_{i+1}\right|\right) \cdot \left|Q_iQ_{i+1}\right| & (g > 0) \\ f_i = \frac{1}{2}|O_iQ_i| \cdot |Q_iP_i| + \frac{1}{2}\left|O_{i+1}Q_{i+1}\right| \cdot \left|P_iQ_{i+1}\right| & (g < 0) \end{cases} & (1 \le i \le m) \\ f_{m+1} = \frac{1}{2}\left|O_{m+1}Q_{m+1}\right| \cdot \left|Q_{m+1}P_{m+1}\right| \end{cases} \tag{14}$$

The initial residual stress remains only in the elastic region of the first valid bending, which shifts the point O_1 to O_1' or O_1'', as shown in Figure 6, thereby changing the total residual stress after levelling. The calculation method is to superimpose the remaining initial residual stress and the rolling residual stress in the region OO_1Q after the rolling residual stress is determined and then correct to f_0.

6. Influence of the Intermesh of Work Rolls on Residual Stress

The residual stress is closely related to the elastoplastic deformation of the sheet, in which the plastic deformation controlled by the intermesh of the work rolls plays a decisive role. The multi-roll levelling parameters discussed in this article are listed in Table 1.

Table 1. Multi-roll levelling parameters.

Parameter	Value
Number of work rolls	11
Diameter of work rolls (mm)	280
Distance between work rolls (mm)	300
Yield stress (MPa)	127.6
Elastic Modulus (GPa)	115.9
Thickness of the sheet (mm)	20
Width of the sheet (mm)	3000
Absolute mean value of initial residual stress (MPa)	40

During the multi-roll levelling process of the sheet, the plastic deformation caused by the work rolls at the entry of the leveller is large due to the large intermesh, plastic deformation caused by the work rolls at the exit is small due to the small intermesh, and even the deformation is elastic. Therefore, the intermesh of the work rolls at the entry is adjusted to control the plastic deformation and to make

the residual stress as small as possible. Additionally, the intermesh of the work rolls at the exit is adjusted to make the residual curvature close to zero.

The plastic deformation is typically the largest caused by the second or third work roll at the entry and then gradually decreases. The influence of the intermesh of the work rolls at the entry on the maximum plastic deformation ratio (the ratio of the thickness of the plastic deformation zone to the total thickness of the sheet metal) based on the coupled curvature integral model is shown in Figure 7. As the intermesh of the work rolls at the entry increases, the maximum plastic deformation ratio of the sheet increases, which makes the elimination of the initial residual stress more sufficient, but the rolling residual stress increases accordingly.

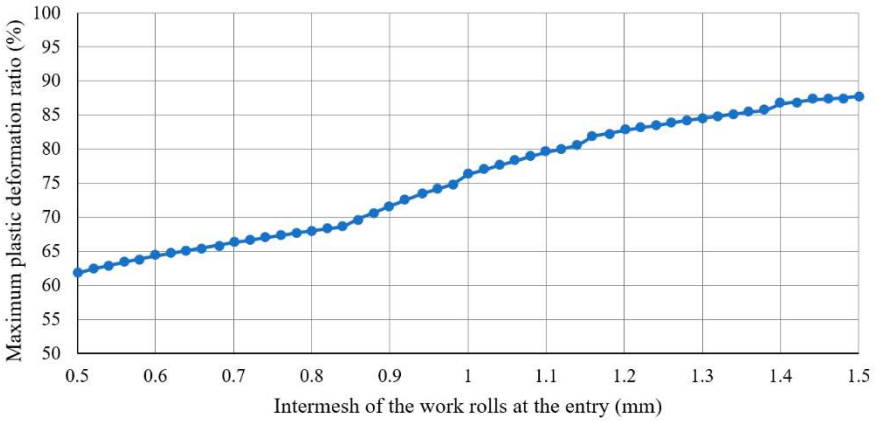

Figure 7. Influence of the intermesh of the work rolls at the entry on the maximum plastic deformation ratio.

The variation of the residual stress calculated by the model described in Section 4 with the intermesh of the work rolls at the entry in the levelling is shown in Figure 8, where the total residual stress is the sum of the rolling residual stress and the remaining initial residual stress. Figure 8 shows that, as the intermesh of the work rolls at the entry increases, the rolling residual stress increases due to the large plastic deformation, but the remaining initial residual stress decreases. The result is a reduction in total residual stress after levelling, with the absolute mean value decreasing from 40 MPa before levelling to 18.5 MPa.

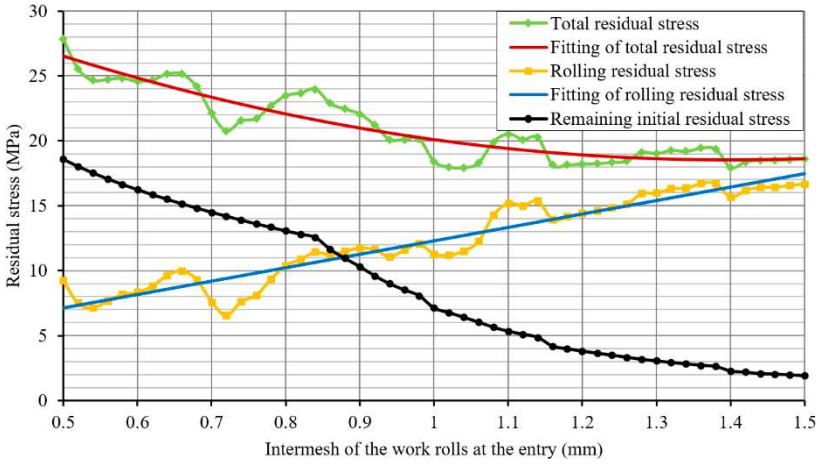

Figure 8. Variation of the residual stress with the intermesh of the work rolls at the entry.

7. Discussions

The results show that the multi-roll levelling could reduce or eliminate the initial residual stress and also cause new rolling residual stresses. The portion of the initial residual stress in the elastic region was not changed and the portion in the plastic region was completely eliminated. The large plastic deformation caused by the large intermesh of the work rolls at the entry was beneficial to the complete elimination of the initial residual stress, but the rolling residual stress increased at the same time. Therefore, if the main purpose of the multi-roll levelling is to eliminate the initial residual stress of the sheet, the intermesh of the work rolls at the entry should be appropriately increased, and if the main purpose is to eliminate the longitudinal bow of the sheet, the intermesh should be appropriately reduced to avoid excessive residual curvature sensitivity.

Besides, the proposed method reveals the evolution mechanism of the residual stress in multi-roll levelling. If combined with the data acquired from different smart sensors, it may help to achieve real-time adjustment of levelling parameters aimed at minimising residual stress. This is one of the steps to fulfilling the intelligent control of the multi-roll levelling lines, which is also a typical application of Industry 4.0 and Intelligent Manufacturing.

The limitation of this method is that the sheet should be an isotropic single plastic material. If it involves allotropic or multiphase materials, the material properties may vary along the thickness of the sheet and stratified cumulative calculation may be needed to solve this problem, in addition, the situation is more complicated if the material is anisotropy, which still needs to be investigated.

8. Conclusions

Accurate analysis of the residual stress evolution in multi-roll levelling of a sheet metal plays an important role in the design of the levellers and the adjustment of the process parameters. Therefore, an analysis method of the residual stress evolution based on the curvature coupling was studied in this article. The absolute mean value of the residual stress in the thickness direction of the sheet was established as the evaluation criterion for the residual stress after levelling. The evolution of residual stress during the first and subsequent multiple bendings of the sheet in multi-roll levelling was analysed. On this basis, the calculation model of the residual stress of the sheet after levelling was established and the influence of the intermesh of the work rolls and the plastic deformation of the sheet on the residual stress was studied.

Author Contributions: Methodology, G.Y. and J.X.; investigation, G.Y. and C.W.; software and validation, Y.L. and C.W.; writing—original draft preparation, G.Y. and C.W.; writing—review and editing, G.Y. and Y.L.

Funding: This research was funded by the National Key R&D Program of China, grant number 2018YFB1701601 and the National Natural Science Foundation of China, grant number 51875515.

Conflicts of Interest: The authors declare no conflict of interest.

References

1. Uppgård, T. *Estimation of Post-Rolling Effects in Cold Rolled Aluminium Strips*; Örebro University: Örebro, Sweden, 2008; p. 136.
2. Fischer, F.D.; Rammerstorfer, F.G.; Friedl, N.; Wieser, W. Buckling phenomena related to rolling and levelling of sheet metal. *Int. J. Mech. Sci.* **2000**, *42*, 1887–1910. [CrossRef]
3. Lopez, C.; Garcia, D.F.; Usamentiaga, R.; Gonzalez, D.; Gonzalez, J.A. Real time system for flatness inspection of steel strips. In Proceedings of the Machine Vision Applications in Industrial Inspection XIII, San Jose, CA, USA, 24 February 2005; Volume 5679, pp. 228–238. [CrossRef]
4. Abdelkhalek, S.; Montmitonnet, P.; Legrand, N.; Buessler, P. Manifested flatness predictions in thin strip cold rolling. *Int. J. Mater. Form.* **2008**, *1*, 339–342. [CrossRef]
5. Abdelkhalek, S.; Montmitonnet, P.; Legrand, N.; Buessler, P. Coupled approach for flatness prediction in cold rolling of thin strip. *Int. J. Mech. Sci.* **2011**, *53*, 661–675. [CrossRef]

6. Kang, Z.W.; Chen, T.C. Longitudinal residual warpage of strip in continuous annealing line. *Appl. Therm. Eng.* **2014**, *62*, 1–12. [CrossRef]
7. Abdelkhalek, S.; Zahrouni, H.; Legrand, N.; Potier-Ferry, M. Post-buckling modeling for strips under tension and residual stresses using asymptotic numerical method. *Int. J. Mech. Sci.* **2015**, *104*, 126–137. [CrossRef]
8. Liu, Z.F.; Wang, Y.Q.; Yan, X.C. A new model for the plate leveling process based on curvature integration method. *Int. J. Mech. Sci.* **2012**, *54*, 213–224. [CrossRef]
9. Grüber, M.; Hirt, G. Investigation of correlation between material properties, process parameters and residual stresses in roller levelling. *Procedia Manuf.* **2018**, *15*, 844–851. [CrossRef]
10. Grüber, M.; Hirt, G. A strategy for the controlled setting of flatness and residual stress distribution in sheet metals via roller levelling. *Procedia Eng.* **2017**, *207*, 1332–1337. [CrossRef]
11. Wang, D.C. Entry and Exit Stress Variation of Cold Rolling Strip. *J. Iron Steel Res. Int.* **2012**, *19*, 19–24. [CrossRef]
12. Xue, J.A.; Hu, X.L.; Liu, X.; Wang, G.D. Mathematical model of elastic-plastic bending for roller leveling. *J. Iron Steel Res.* **2008**, *20*, 33–36.
13. Liu, Z.F.; Wang, Y.Q.; Ou, H.G.; Yan, X.C.; Luo, Y.X. An analytical leveling model of curvature and residual stress simulation for H-beams. *J. Constr. Steel Res.* **2014**, *102*, 13–23. [CrossRef]
14. Doege, E.; Menz, R.; Huinink, S. Analysis of the levelling process based upon an analytic forming model. *CIRP Ann.-Manuf. Technol.* **2002**, *51*, 191–194. [CrossRef]
15. Weiss, M.; Rolfe, B.; Hodgson, P.D.; Yang, C.H. Effect of residual stress on the bending of aluminium. *J. Mater. Process. Technol.* **2012**, *212*, 877–883. [CrossRef]
16. Nakhoul, R.; Montmitonnet, P.; Legrand, N. Manifested flatness defect prediction in cold rolling of thin strips. *Int. J. Mater. Form.* **2015**, *8*, 283–292. [CrossRef]
17. Mathieu, N.; Potier-Ferry, M.; Zahrouni, H. Reduction of flatness defects in thin metal sheets by a pure tension leveler. *Int. J. Mech. Sci.* **2017**, *122*, 267–276. [CrossRef]
18. Abvabi, A.; Rolfe, B.; Hodgson, P.D.; Weiss, M. The influence of residual stress on a roll forming process. *Int. J. Mech. Sci.* **2015**, *101*, 124–136. [CrossRef]
19. Tiwari, A.K.; Patel, A.R.; Kumar, N. Investigation of strain rate on residual stress distribution. *Mater. Des.* **2015**, *65*, 1041–1047. [CrossRef]
20. Singh, A.; Agrawal, A. Investigation of surface residual stress distribution in deformation machining process for aluminum alloy. *J. Mater. Process. Technol.* **2015**, *225*, 195–202. [CrossRef]
21. Sun, Y.; Luzin, V.; Daniel, W.J.T.; Meehan, P.A.; Zhang, M.; Ding, S. Development of the slope cutting method for determining the residual stresses in roll formed products. *Measurement* **2017**, *100*, 26–35. [CrossRef]
22. Quach, W.M.; Teng, J.G.; Chung, K.F. Residual stresses in steel sheets due to coiling and uncoiling: A closed-form analytical solution. *Eng. Struct.* **2004**, *26*, 1249–1259. [CrossRef]
23. Quach, W.M.; Teng, J.G.; Chung, K.F. Residual stresses in press-braked stainless steel sections, I: Coiling and uncoiling of sheets. *J. Constr. Steel Res.* **2009**, *65*, 1803–1815. [CrossRef]
24. Silvestre, E.; Garcia, D.; Galdos, L.; de Argandona, E.S.; Mendiguren, J. Roll levelling semi-analytical model for process optimization. *J. Phys. Conf. Ser.* **2016**, *734*, 032034. [CrossRef]
25. Silvestre, E.; de Argandona, E.S.; Galdos, L.; Mendiguren, J. Testing and modeling of roll levelling process. *Key Eng. Mater.* **2014**, *611–612*, 1753–1762. [CrossRef]
26. Nakhoul, R.; Montmitonnet, P.; Potier-Ferry, M. Multi-scale method for modeling thin sheet buckling under residual stresses in the context of strip rolling. *Int. J. Solids Struct.* **2015**, *66*, 62–76. [CrossRef]
27. Tan, Z.; Li, W.B.; Persson, B. On Analysis and Measurement of Residual-Stresses in the Bending of Sheet Metals. *Int. J. Mech. Sci.* **1994**, *36*, 483–491. [CrossRef]
28. Zhang, S.Y.; Wu, Y.X.; Gong, H. A modeling of residual stress in stretched aluminum alloy plate. *J. Mater. Process. Technol.* **2012**, *212*, 2463–2473. [CrossRef]
29. Milenin, A.; Kustra, P.; Kuziak, R.; Pietrzyk, M. Model of residual stresses in hot-rolled sheets with taking into account relaxation process and phase transformation. *Procedia Eng.* **2014**, *81*, 108–113. [CrossRef]
30. Abvabi, A.; Rolfe, B.; Hodgson, P.D.; Weiss, M. An inverse routine to predict residual stress in sheet material. *Mater. Sci. Eng. S-Struct.* **2016**, *652*, 99–104. [CrossRef]
31. Liu, B.; Villavicencio, R.; Guedes Soares, C. Experimental and numerical analysis of residual stresses and strains induced during cold bending of thick steel plates. *Mar. Struct.* **2018**, *57*, 121–132. [CrossRef]

32. Mehner, T.; Bauer, A.; Härtel, S.; Awiszus, B.; Lampke, T. Residual-stress evolution of cold-rolled DC04 steel sheets for different initial stress states. *Finite Elem. Anal. Des.* **2018**, *144*, 76–83. [CrossRef]
33. Milenin, A.; Kuziak, R.; Lech-Grega, M.; Chochorowski, A.; Witek, S.; Pietrzyk, M. Numerical modeling and experimental identification of residual stresses in hot-rolled strips. *Arch. Civ. Mech. Eng.* **2016**, *16*, 125–134. [CrossRef]
34. Li, S.Z.; Yin, Y.D.; Xu, J.; Hou, J.M.; Yoon, J.H. Numerical simulation of continuous tension leveling process of thin strip steel and its application. *J. Iron Steel Res. Int.* **2007**, *14*, 8–13. [CrossRef]
35. Tran, D.C.; Tardif, N.; Limam, A. Experimental and numerical modeling of flatness defects in strip cold rolling. *Int. J. Solids Struct.* **2015**, *69–70*, 343–349. [CrossRef]
36. Tran, D.C.; Tardif, N.; El Khaloui, H.; Limam, A. Thermal buckling of thin sheet related to cold rolling: Latent flatness defects modeling. *Thin Walled Struct.* **2017**, *113*, 129–135. [CrossRef]
37. Cui, L.; Shi, Q.Q.; Liu, X.H.; Hu, X.L. Residual Curvature of Longitudinal Profile Plate Roller in Leveling Process. *J. Iron Steel Res. Int.* **2013**, *20*, 23–27. [CrossRef]
38. Cui, L.; Hu, X.L.; Liu, X. Analysis of roll bending for plate roller leveling. *J. Iron Steel Res.* **2012**, *24*, 6–10.
39. Cui, L.; Hui, X.L.; Liu, X.H. Analysis of Leveling Strategy for a plate Mill. *Adv. Mater. Res.-Switz.* **2011**, *145*, 424–428. [CrossRef]
40. Tanner, D.A.; Robinson, J.S. Modelling stress reduction techniques of cold compression and stretching in wrought aluminium alloy products. *Finite Elem. Anal. Des.* **2003**, *39*, 369–386. [CrossRef]
41. Wawszczak, R.; Baczmański, A.; Braham, C.; Seiler, W.; Wróbel, M.; Wierzbanowski, K.; Lodini, A. Residual stress field in steel samples during plastic deformation and recovery processes. *Philos. Mag.* **2011**, *91*, 2263–2290. [CrossRef]
42. Withers, P.J.; Bhadeshia, H.K.D.H. Residual stress. Part 1—Measurement techniques. *Mater. Sci. Technol.* **2001**, *17*, 355–365. [CrossRef]
43. Skvortsov, V.F.; Boznak, A.O.; Kim, A.B.; Arlyapov, A.Y.; Dmitriev, A.I. Reduction of the residual stresses in cold expanded thick-walled cylinders by plastic compression. *Def. Technol.* **2016**, *12*, 473–479. [CrossRef]
44. Koç, M.; Culp, J.; Altan, T. Prediction of residual stresses in quenched aluminum blocks and their reduction through cold working processes. *J. Mater. Process. Technol.* **2006**, *174*, 342–354. [CrossRef]
45. Umemoto, T. Residual stress generation and control. *Bull. Jpn. Inst. Met.* **1990**, *29*, 973–980. [CrossRef]
46. Fumio, H. The corrective effect of roller leveler. *J. JSTP* **1961**, *2*, 359.